

## Enhanced Cr(VI) removal using iron nanoparticle decorated graphene

Humera Jabeen,<sup>§</sup> Vimlesh Chandra,<sup>§</sup> Sehoon Jung, Jung Woo Lee, Kwang S. Kim,\* and Seung Bin Kim\*

## Supporting Information

### Chemicals

Graphite powder (300 mesh, purity 99.9999%) was supplied by the Alpha Aesar. Potassium permanganate (99+ %) was obtained from Sigma Aldrich and Potassium di chromate (99.95%) from Aldrich. Shinyo pure chemicals Japan was the supplier of Iron(III) chloride hexahydrate. The hydrogen peroxide, sodium borohydride, Phosphoric acid (85%) and sulphuric acid were purchased by Samchun Chemicals, Korea. Hydrochloric acid was obtained from Merck Germany. All chemicals were used directly as received and stock solutions were prepared by using doubly deionized water (18MΩ Milli-Q).

### Synthesis of Graphene Oxide (GO)

Graphite powder was oxidized by a mixture of acids and additional amount of Potassium permanganate as described in improved synthesis of graphene oxide. In brief a 9:1 mixture of H<sub>2</sub>SO<sub>4</sub> (95%) / H<sub>3</sub>PO<sub>4</sub> (85%) [360:40 mL] was added to a mixture of graphite powder (3.0 g, 1 wt. equiv.) and KMnO<sub>4</sub> (18.0 g; 6 wt. equiv). It was an exothermic reaction, producing heat to raise temperature up to 40°C. It was stirred for 24 hours at 50°C. Then it was cooled to room temperature and poured onto ice (~ 400 mL) containing 30% H<sub>2</sub>O<sub>2</sub> (15 mL). Supernatant was decanted away after settling overnight. The remaining solid was purified by multiple washings with some modifications. First it was stirred and kept overnight with 30% HCl (200 mL) and then 15% HCl (200 mL) to remove metal ions impurities. The mixture was centrifuged for 30 minutes at 4000 rpm and washed for the removal of HCl with DI water several times till the pH of solution was approximately 4.0 or above. Finally the solid was neutralized by centrifuging it with pure ethanol two times. Ethanol was removed by rotary vacuum evaporation and dried at room temperature overnight in vacuum oven to get graphene oxide powder for further use.

### Synthesis of reduced graphene oxide (RGO)

Graphene oxide (300 mg/300 mL) was dispersed in DI water by 1 hour ultrasonication. NaBH<sub>4</sub> solution (5 g/80 mL; 1.65 M) was taken in dropping funnel. Then flask solution was heated up to 90°C and sodium borohydride was carefully added dropwise very slowly; then, whole contents in the flask turned black. It was rapidly stirred at 90°C for 4 hours; solution was cooled to room temperature. This black solution was filtered, washed with water and then with ethanol several times. Finally, it was dried in vacuum-oven over night to get black shiny solid.

### Synthesis of iron nanoparticles decorated graphene (G-nZVI)

Required amount of graphene oxide (Table 1) was dispersed in DI water by 1 hour ultrasonication bath. FeCl<sub>3</sub>·6H<sub>2</sub>O (2.703 g/20 mL; 1 M) solution was added in GO and further sonicated for 1 hour in Ar atm. NaBH<sub>4</sub> solution (5 g/80 mL; 1.65 M) was taken in dropping funnel and made it oxygen free by flowing argon gas. This was added slowly to reduce iron ions and graphene oxide at 90°C. Whole contents turned jet black at once with brisk evolution of gases. The reaction was stopped after 4 hours and cooled down up to room temperature in Ar gas protection. This black solution was filtered, washed with water and then with ethanol several times and dried in vacuum at 50°C for 24 hours.

**Table 1. Wt % Graphene oxide loading in FeCl<sub>3</sub>·6H<sub>2</sub>O to synthesize G-nZVI**

Sample Name	FeCl <sub>3</sub> ·6H <sub>2</sub> O (g/mL)	GO (g/mL)	NaBH <sub>4</sub> (g/mL)
1.2 wt%	2.703/20	0.03375/300	5/80
6wt%	2.703/20	0.1486/300	5/80
11wt%	2.703/20	0.300/300	5/80
nZVI	2.703/20	- /300	5/80

### Synthesis of iron nanoparticles (nZVI)

Zerovalent iron nanoparticles (nZVI) were prepared with the same method as stated above, except graphene oxide addition.

### Analysis Instruments

XRD patterns of Iron nanoparticles and graphene-iron composites were obtained by using a Rigaku,D/Max-2500 Powder X-Ray Diffractometer at 40 Kev and 30 mA with a step size of 2° with Cu K $\alpha$  radiation ( $\lambda = 1.54056 \text{ \AA}$ ). FTIR spectra were recorded, using a Bomem DA8

spectrometer at room temperature. Powder samples for DRIFTS were used for infrared spectra. Raman spectra were obtained for 500-2000 cm<sup>-1</sup> using Bruker optics model Senterra employing 532 nm wavelength incident laser light and power 20 mW. Scanning Electron Microscope (SEM) images and EDAX were done by JEOL-JSM-7401F.

Transmission electron microscopy (TEM) and high-resolution transmission electron microscopy (HRTEM) observations were carried out on a JEM-2100F (Cs corrected STEM) electron microscope with an accelerating voltage of 200 kV. The Chromium concentrations before and after adsorption were determined by an inductively coupled plasma- atomic emission spectrometer (ICP-AES) (Spectra Flame Modulae). Magnetic measurements were performed on powder samples using a Quantum Design MPMS-XL -7 magnetometer. Zero-field cooled (ZFC) and field-cooled (FC) magnetization curves were recorded for 5–300 K temperature range with an applied magnetic field of 200 Oe. XPS analysis was made with an ESCALAB-220I-XL (THERMO-ELECTRON, VG Company) device. Photoemission was stimulated by a nonmonochromatized Mg K $\alpha$  source (1253.6 eV) for all samples. Surface area was measured using micromeritics ASAP 2010. AFM images were taken on SPM System (AFM/STM Base) VEECO Dimension 3100 + Nanoscope V (Version 7.0). The pH was measured by an Orion 3 star pH meter.

### Adsorption experiments

Potassium dichromate ( $K_2Cr_2O_7$ , FW 294.19) was used as the source of Cr (VI). A stock solution (2 mM) was prepared in distilled water by dissolving 591.208 mg of potassium dichromate in DI water. Removal efficiency (E) of chromium ions was calculated by measuring the chromium concentration before and after adsorption, respectively. The adsorbent dosage of G-nZVI and nZVI applied in the present work was 0.2 g/L. For evaluation of reduction and adsorption efficacy, adsorbents were added into 50 mL of chromium solution and sonicated for 10.0 minutes and stirred for 4 hours at room temperature. At the end of reduction/adsorption, the suspension was separated by using magnet. The chromium concentrations, prior to and after adsorption, were determined by an inductively coupled plasma-atomic emission spectrometer (ICP-AES).

Adsorption isotherms were studied by monitoring Cr(VI) solution of 25 ppm – 125 ppm under a similar condition of temperature 20°C, pH = 4.25 and adsorption time 4 hour. The data of chromium adsorption was fitted using *Freundlich* [6] and *Langmuir isotherm* models [7] and listed in Table 2.

The Langmuir isotherm is expressed as

$$q_e = abC_e / (1 + bC_e) \quad \text{S1}$$

and Freundlich isotherm is represented by

$$q_e = k (C_e)^{1/n} \quad \text{S2}$$

where  $q_e$  is the amount of chromium adsorbed per unit weight of adsorbent (mg/g),  $C_e$  is the equilibrium concentration of chromium (mg/L),  $b$  is the constant related to the free energy of adsorption (l/mg), and  $a$  is the maximum adsorption capacity (mg/g). Freundlich constant ( $k$ ) is indicative of the relative adsorption capacity of the adsorbent (mg/g), and  $(1/n)$  is the adsorption intensity.

**Table 2. Langmuir and Freundlich adsorption isotherm parameters for chromium removal on nZVI and G-nZVI**

Isotherm Type	Isotherm Cons.	nZVI	G-nZVI
Langmuir	a (mg/g)	148.79	162.59
	b (l/mg)	0.034	0.045
	R <sup>2</sup>	0.99	0.98
Freundlich	k	24.4	35.99
	n	2.97	3.57
	R <sup>2</sup>	0.99	0.993

The adsorption kinetics was done for 100 ppm Cr(VI) ion solution at pH = 4.25, T = 20°C. The kinetic data were fitted for pseudo second-order kinetic model to describe Cr<sup>6+</sup> adsorption on the nZVI and G-nZVI. The equation is expressed as

$$t/q_t = 1/q_e^2 k_2 + 1/q_e t \quad \text{S3}$$

Where  $q_t$  and  $q_e$  are the amounts (mg/g) of Cr (VI) adsorbed at time  $t$  and at equilibrium, respectively, and  $k_2$  (g/mg·min) is the equilibrium rate constant of pseudo second-order adsorption. The initial adsorption rate  $V_0 = k_2 q_e^2$ , and  $q_e$  for chromium adsorption parameters

were calculated (Table 3). The chromium adsorption on iron and iron decorated graphene is favorable by the pseudo-second order kinetics.

**Table3: Parameters of a Pseudo-Second-Order Kinetic Model**

Adsorbent	Isotherm Constant	Cr (VI)	R <sup>2</sup>
nZVI	q <sub>e</sub>	123.6	0.987
	k <sub>2</sub>	3.0 x10 <sup>-4</sup>	
	V <sub>0</sub>	4.65	
G-nZVI	q <sub>e</sub>	226.244	0.99
	k <sub>2</sub>	3.1x10 <sup>-4</sup>	
	V <sub>0</sub>	6 .13	

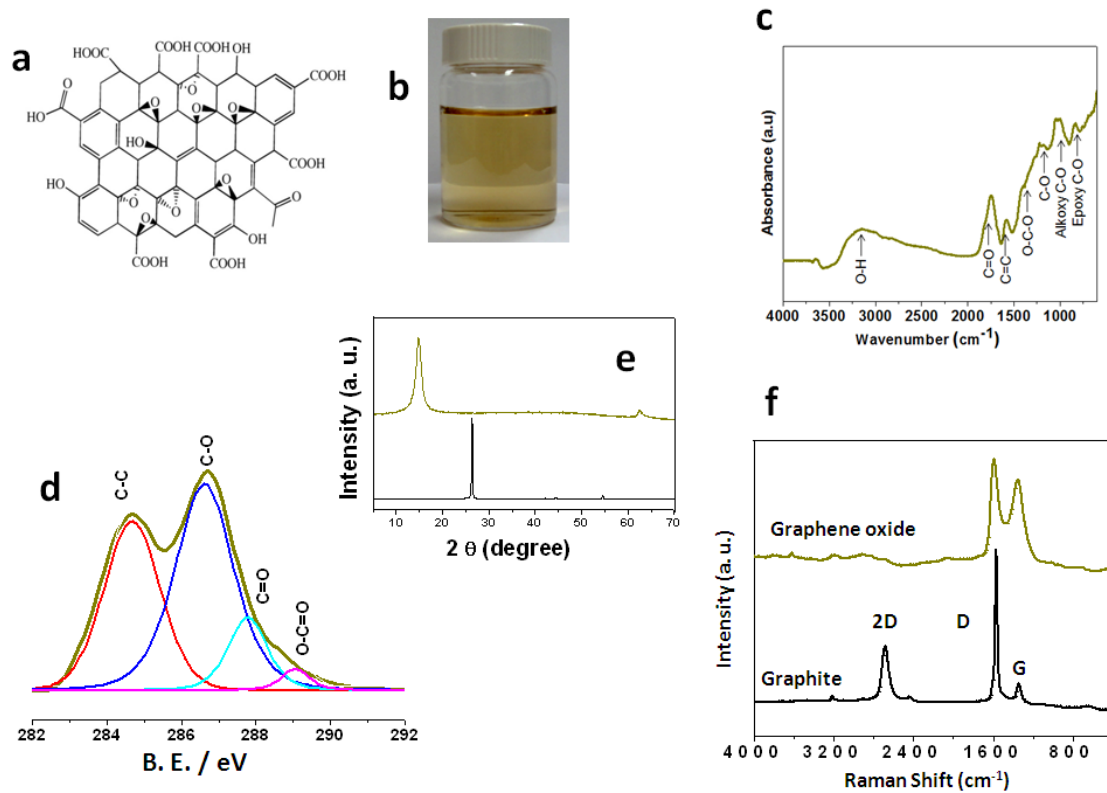


**Fig. S1:** (a) Chemical structure of graphene oxide, (b) aqueous solution of graphene oxide (0.1 mg / ml), (c) FTIR spectra of graphene oxide showing the presence of oxygenated and nonoxygenated functional group, (d) XPS spectra for C1s: Carbon  $\text{sp}^2$  (C=C, 284.6 eV), epoxy/hydroxyls (C-O, 286.7 eV), carbonyl (C=O, 287.8 eV), and carboxylates (O-C=O, 289.2 eV), (e) X-ray diffraction pattern of graphite (black) and graphene oxide (dark yellow), and (f) Raman spectra of graphite (black) and graphene oxide (dark yellow).

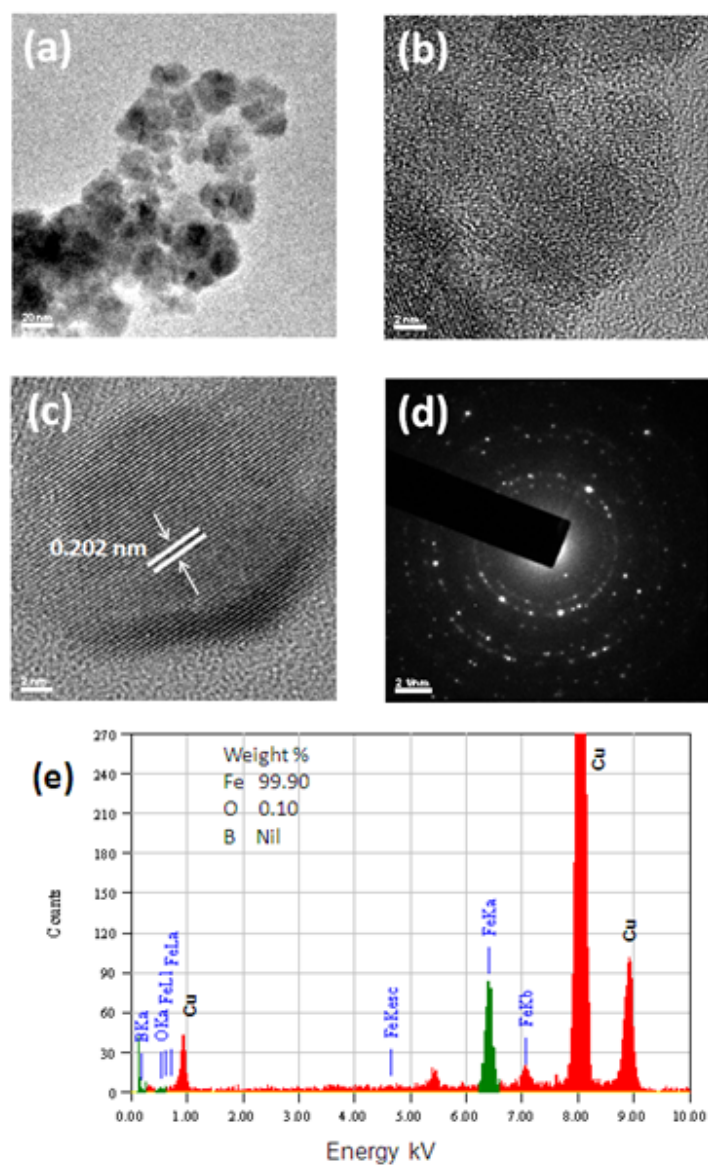


**Fig. S2:** (a-d) TEM images of nZVI particles showing crystalline particles and (e) EDAX analysis showing the presence of oxygen and absence of boron.

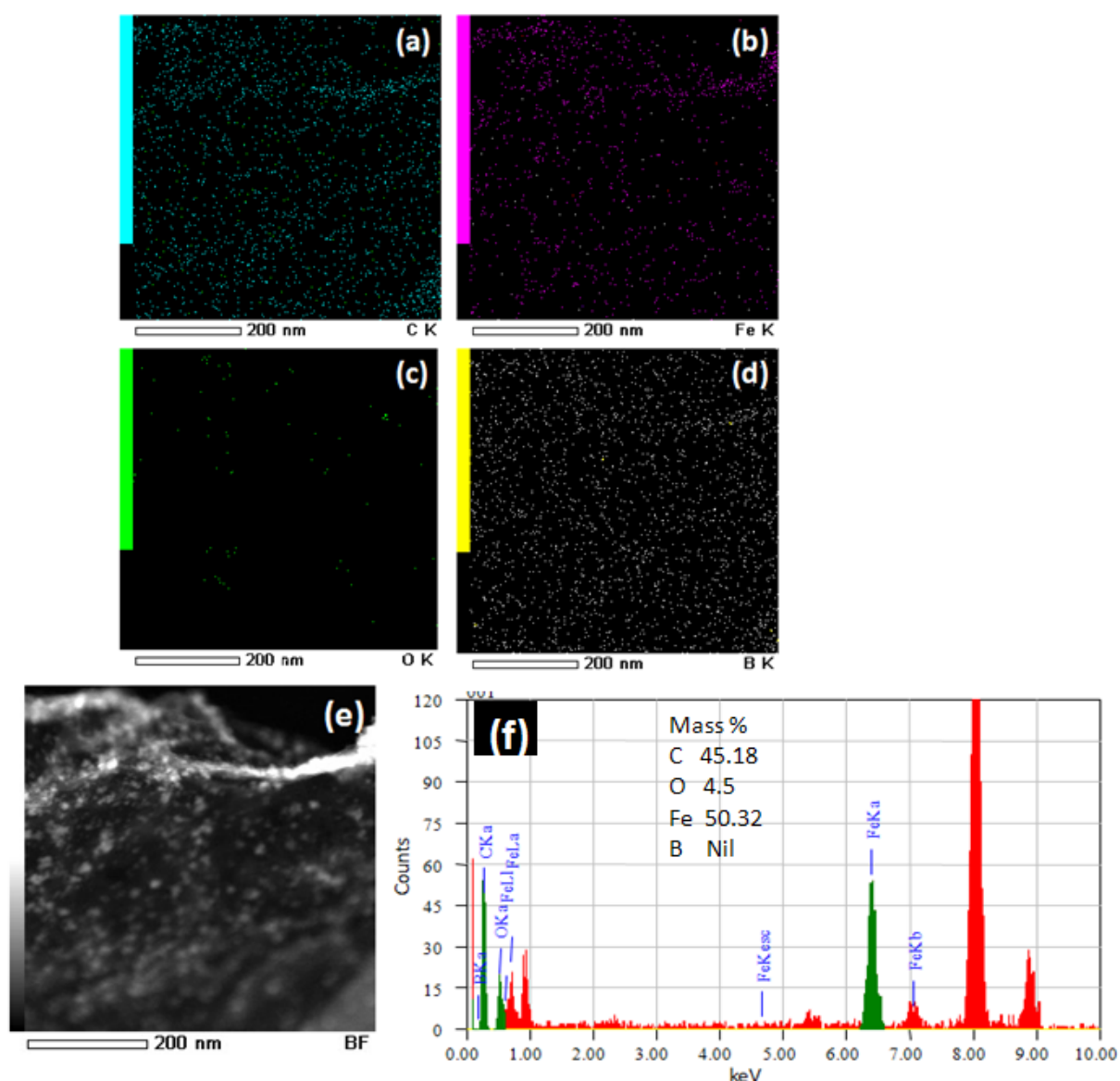


**Fig. S3:** Elemental mapping of iron nanoparticles decorated graphene sheets showing the presence of (a) carbon, (b) iron, (c) oxygen, and (d) the absence of boron, (e) the BF image, and (f) the TEM-EDX patterns of G-nZVI.

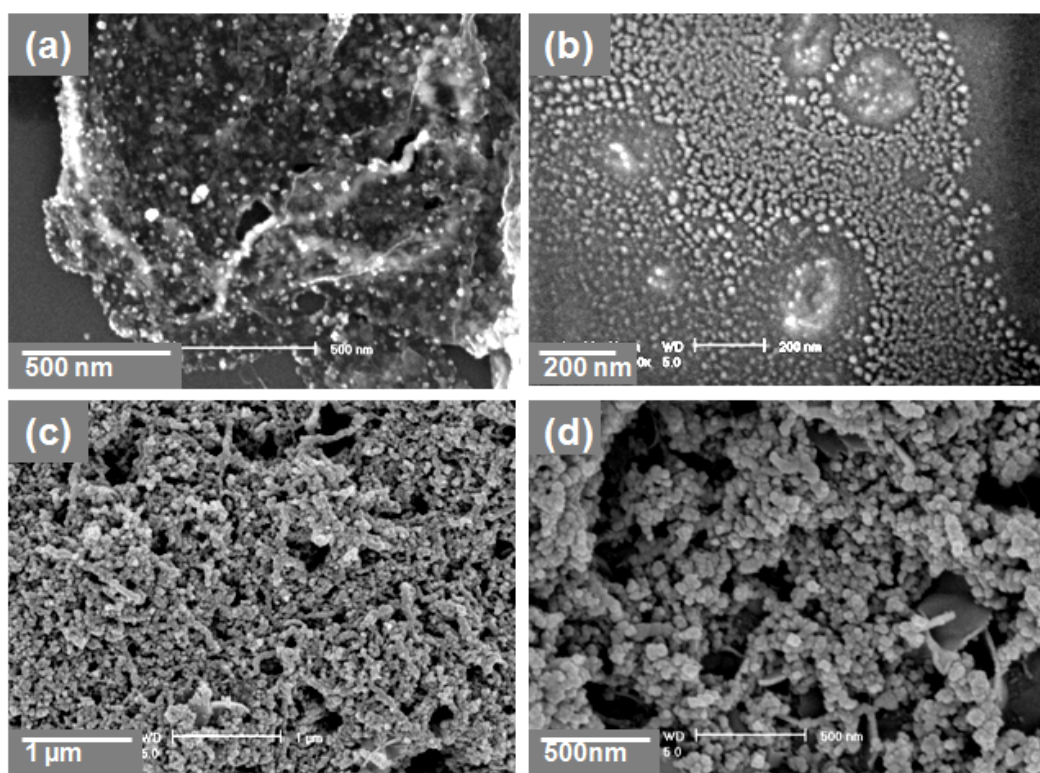


**Fig. S4:** SEM images of (a-b) iron nanoparticles decorated graphene (G-nZVI) and (c-d) bare iron naoparticles (nZVI).

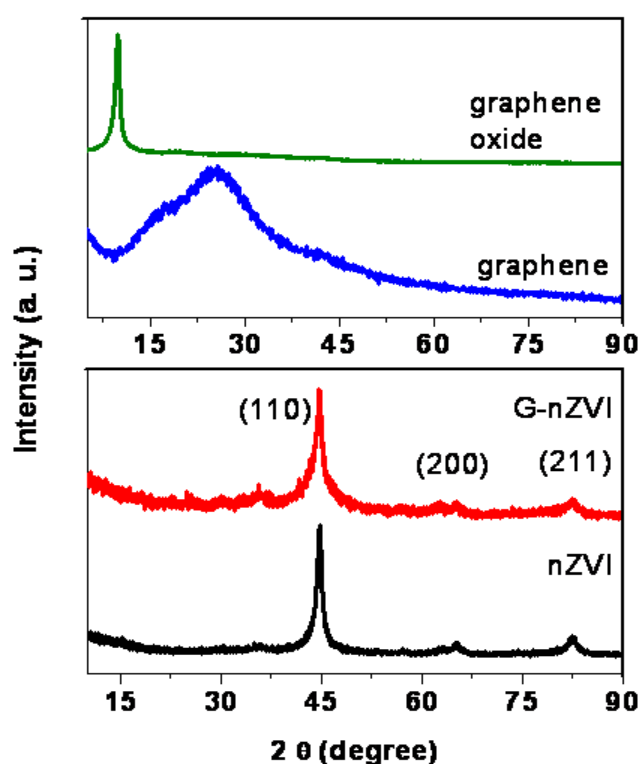


**Fig. S5:** The XRD Pattern of GO shows a large interlayer spacing  $d_{002} = 0.9$  nm for the (002) peak at  $2\theta = 10^\circ$  because of the presence of abundant oxygenated groups and intercalated water molecules after oxidation. Reduction with sodium borohydride removes surface oxide groups and intercalated water, resulting in a drastic decreased distance between sheets ( $d_{002} = 3.4\text{\AA}$  at  $2\theta = 25.6^\circ$  in graphene). The XRD analysis of the iron nanoparticles (nZVI) and iron decorated graphene (G-nZVI) shows broad peaks for  $\alpha\text{-Fe}^\circ$  at the  $2\theta$  of 44.6, 65, and  $82.5^\circ$  with indexes of (110), (200), and (211) (JCPDS No. 0696). The broad peak indicating small particles is further decreased in the presence of graphene sheets.

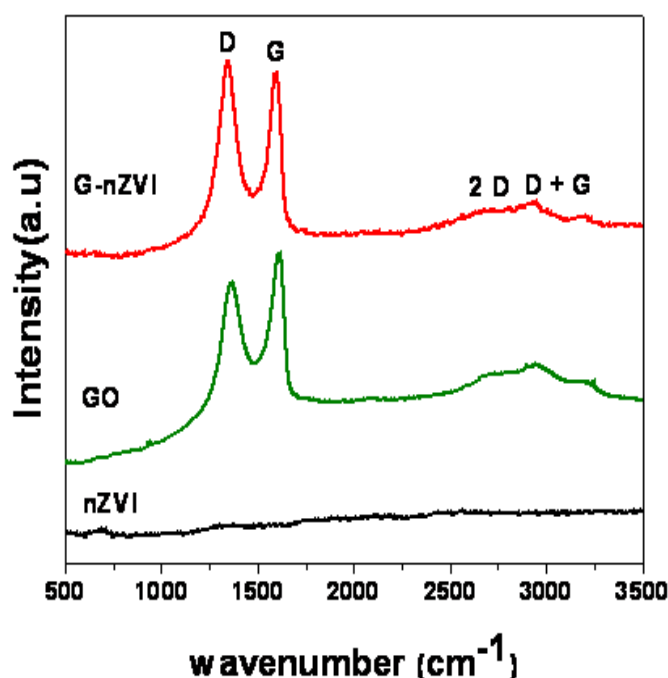


**Fig. S6:** Raman spectrum of bare iron nanoparticles (nZVI) reveals no dominant peak which is characteristic of iron nanoparticles. Only very weak peak around  $700 \text{ cm}^{-1}$  can be seen due to surface oxidation. Raman spectrum of graphene oxide has the G band and D band at  $1612 \text{ cm}^{-1}$   $1366 \text{ cm}^{-1}$ , respectively. The Raman spectra of the iron decorated graphene (G-nVI) is similar to graphene oxide with increased intensity ratio ( $r = I_D/I_G$ ) from 0.89 to 1.1. The 2D band is broadened and doublet in the case of composite and we can see a weak 2D band along with the D+G combination band induced by disorder at  $2916 \text{ cm}^{-1}$ .

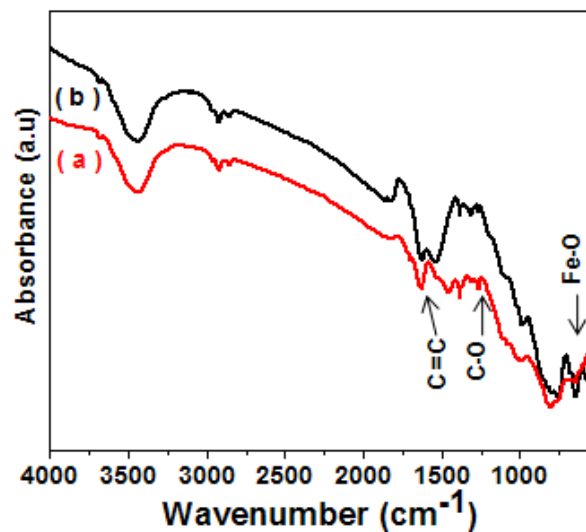


**Fig. S7:** FTIR spectra of iron decorated graphene (Red color) and bare iron nanoparticles (black color).

FTIR spectrum of GO, illustrated in Figure S1(e) confirms the successful oxidation of graphite. The characteristic vibrations are strong, a broad intense band O-H ( $3000 - 3500 \text{ cm}^{-1}$ )  $\text{C}=\text{O}$  ( $1749 \text{ cm}^{-1}$ ), un-oxidized graphitic domains  $\text{C}=\text{C}$  ( $1585 \text{ cm}^{-1}$ ),  $\text{C}-\text{OH}$  ( $1318 \text{ cm}^{-1}$ ), epoxy  $\text{C}-\text{O}$  ( $1228 \text{ cm}^{-1}$ ) and alkoxy  $\text{C}-\text{O}$  ( $1054 \text{ cm}^{-1}$ ) stretches. Most of oxygen containing functional groups, is successfully removed in reduced graphene oxide composite. Reduced G-nZVI composites [Figure S3(a)] show the main peak at  $1586 \text{ cm}^{-1}$  due to aromatic  $\text{C}=\text{C}$  stretch, while low intensity peaks at  $1052 \text{ cm}^{-1}$  due to  $\text{C}-\text{O}$  stretch show residual surface oxygen species which are not completely removed. nZVI spectrum [Figure S3(b)] also shows weak surface oxidation peaks around  $600 \text{ cm}^{-1}$  due to exposure to air.

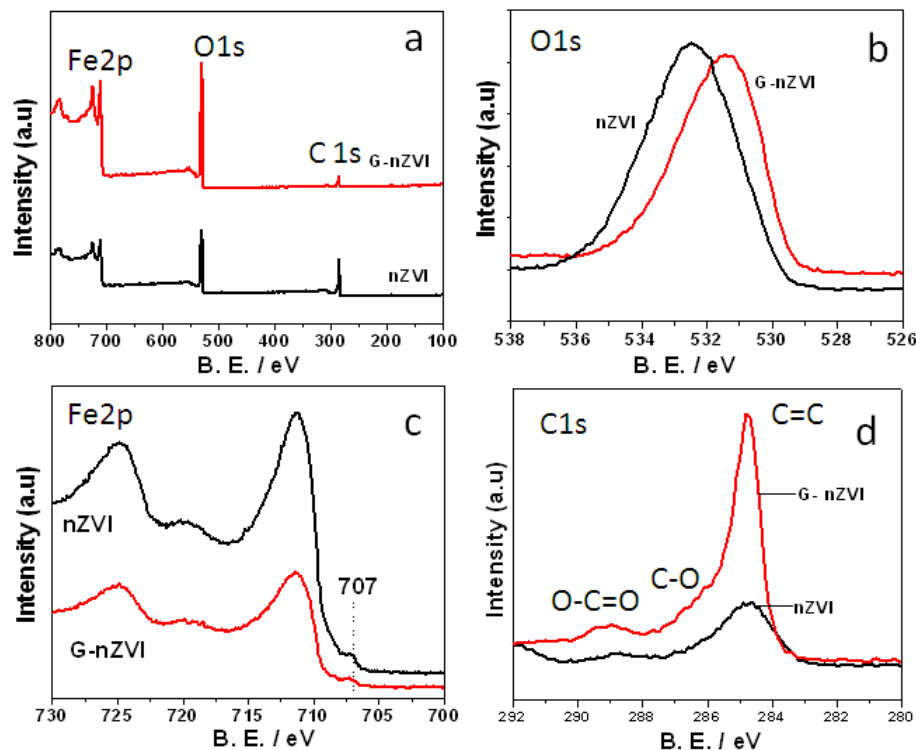


**Fig. S8:** XPS spectra of iron decorated graphene (red color) and bare iron nanoparticles (black color). (a) Full survey, (b) survey for oxygen, (c) survey for iron, and (d) survey for carbon.

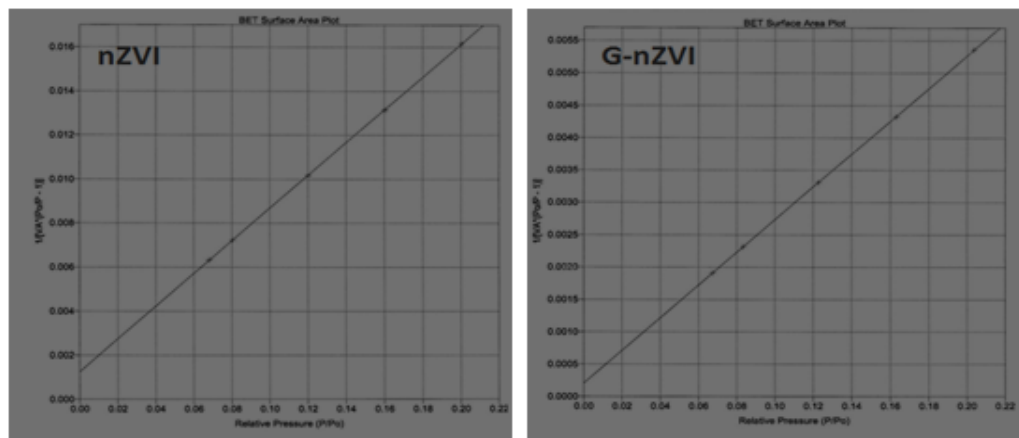


**Fig. S9:** BET surface area of iron nanoparticles and iron decorated graphene sheets.

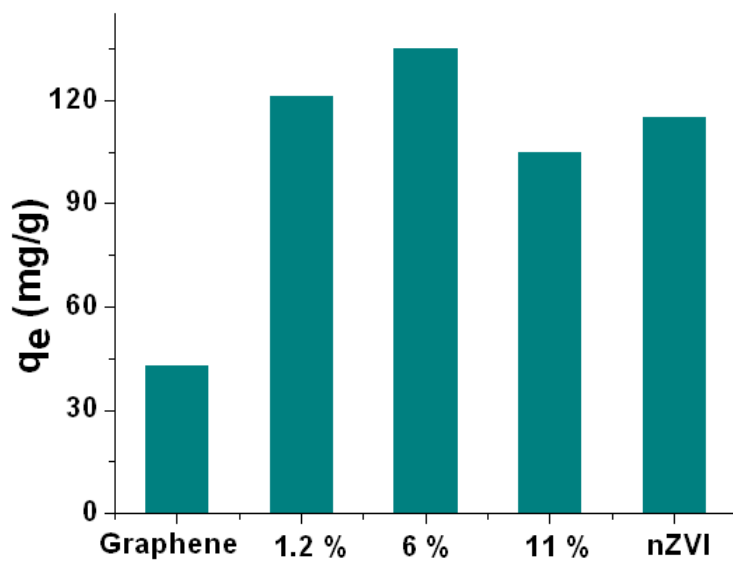


**Fig. S10:** Optimization of graphene oxide loading in iron nanoparticles for chromium adsorption.

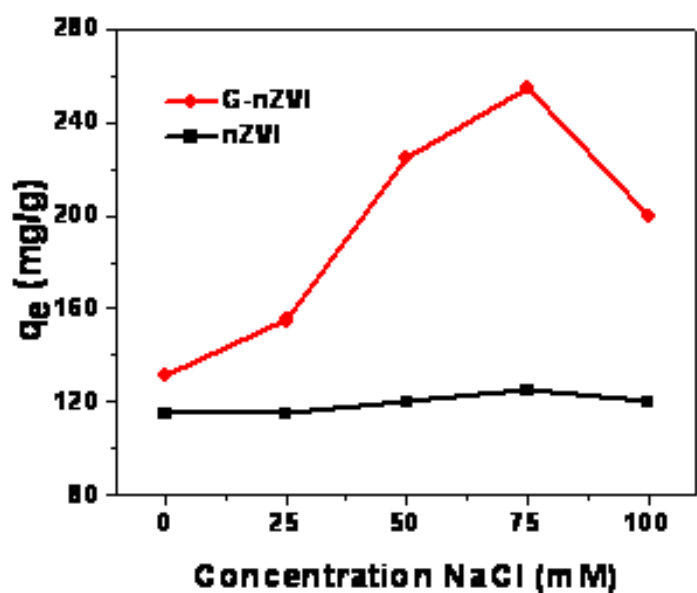


**Fig. S11.** The influence of ionic strength on the absorption of Chromium on to G-nZVI and nZVI.